

High atmospheric CO₂ concentration causes increased respiration by the oxidative pentose phosphate pathway in chloroplasts

Thomas Wieloch

Department of Medical Biochemistry and Biophysics, Umeå University, 90187 Umeå, Sweden

Email: thomas.wieloch@umu.se

Phone: +46706460369

ORCID: 0000-0001-9162-2291

Twitter: <https://twitter.com/WielochThomas>

ResearchGate: <https://www.researchgate.net/profile/Thomas-Wieloch>

GoogleScholar: <https://scholar.google.de/citations?user=g0ZB7JMAAAAJ&hl=de&oi=sra>

Key words: Calvin-Benson cycle, carbon metabolism, CO₂ fertilisation, glucose-6-phosphate shunt, hydrogen stable isotopes, oxidative pentose phosphate pathway, photosynthesis, respiration

Abstract

Despite significant research efforts, the question of whether rising atmospheric CO₂ concentrations (C_a) affect leaf respiration remains unanswered. Here, I reanalyse published hydrogen isotope abundances in starch glucose of sunflower leaves. I report that, as C_a increases from 450 to 1500 ppm, respiration by the oxidative pentose phosphate pathway in chloroplasts increases from 0 to $\approx 5\%$ relative to net carbon assimilation. This is consistent with known regulatory properties of the pathway. Summarising recent reports of metabolic fluxes in plant leaves, a picture emerges in which mitochondrial processes are distinctly less important for overall respiration than the oxidative pentose phosphate pathways in chloroplasts and the cytosol. Regulatory properties of these pathways are consistent with observations of lower-than-expected stimulations of photosynthesis in response to increasing C_a . Reported advances in understanding leaf respiratory mechanisms may enable modelling and prediction of respiration effects (*inter alia*) on biosphere-atmosphere CO₂ exchange and plant performance under climate change.

Introduction

Despite significant research efforts, the question of whether rising atmospheric CO₂ concentration (C_a) affects leaf respiration remains unanswered (Gonzàlez-Meler *et al.*, 2004; Way *et al.*, 2015; Dusenge *et al.*, 2019). A large body of research conveys an entirely inconsistent picture including reports of both positive and negative responses. This may (*inter alia*) be due to methodological difficulties to disentangle overlapping CO₂ fluxes at the tissue level and an incomplete understanding of respiration at the metabolic level with a strong research focus on mitochondrial processes. Overall, leaf respiration has remained a major unknown from the metabolic to the Earth system level.

State-of-the-art isotope techniques enable analyses of specific metabolic fluxes (Ehlers *et al.*, 2015; Wieloch *et al.*, 2021b; Xu *et al.*, 2022; Wieloch *et al.*, 2022c). Recently, we reported two deuterium fractionation signals (i.e., systematic variability in deuterium abundance) in starch glucose of sunflower leaves (Wieloch *et al.*, 2022a). A signal at glucose H¹ reflects hydrogen isotope fractionation by chloroplast glucose-6-phosphate dehydrogenase (**G6PD**) and associated flux through the oxidative pentose phosphate pathway (**OPPP**, Fig. 1A). This anaplerotic pathway feeds pentose phosphates into the Calvin-Benson cycle (**CBC**), supplies NADPH, and releases CO₂. Another signal at glucose H² reflects hydrogen isotope fractionation by chloroplast phosphoglucose isomerase (**PGI**) and associated shifts of the reaction catalysed by PGI from kinetic to equilibrium conditions.

Here, these fractionations at glucose H¹ and H² are respectively expressed as

$$\delta D_1 = \frac{D_1}{D_{6S}} - 1 \quad \text{Eqn 1}$$

and

$$\delta D_2 = \frac{D_2}{D_{6R}} - 1 \quad \text{Eqn 2}$$

where D_i denotes relative deuterium abundances at specific carbon-bound hydrogens of glucose. In these equations, deuterium abundances at glucose H^{6S} and H^{6R} are used as references because glucose H¹ and H^{6S} and H² and H^{6R} have the same precursors at the chloroplast triose-phosphate level, and H^{6S} and H^{6R} are not modified in the starch biosynthesis pathway (Wieloch *et al.*, 2022a). In these notations, increases of δD_1 above zero reflect increases in anaplerotic flux into the CBC while increases of δD_2 from negative to positive values reflect shifts of the PGI reaction from being on the side of F6P over being at equilibrium to being on the side of G6P (Wieloch *et al.*, 2022a).

Previously, we investigated these processes in leaves of sunflowers raised over 7–8 weeks at $C_a = 450$ ppm (Wieloch *et al.*, 2022a). We reported evidence against anaplerotic flux under these conditions. However, moving the plants into a low- C_a atmosphere for two days led to significant increases in δD_1 and δD_2 consistent with an increase in anaplerotic flux and a shift of the PGI reaction from kinetic to equilibrium conditions, respectively (see reanalysis of previous low- C_a results based on equations 1 and 2 in Supporting Information Notes S1). Related fractionation signals were also found in the starch derivative tree-ring glucose under drought (Wieloch *et al.*, 2018, 2022b).

Here, I reanalyse our previously published data (Wieloch *et al.*, 2022a) to assess how metabolism behaves after moving the plants into a high- C_a atmosphere for two days. I report that, as C_a increases from 450 to 1500 ppm, respiration by the OPPP in chloroplasts increases from 0 to $\approx 5\%$ relative to the rate of net carbon assimilation. This is consistent with known regulatory properties of the pathway. Summarising recent reports of metabolic fluxes in plant leaves, a picture emerges in which mitochondrial processes seem distinctly less important for overall respiration than the oxidative pentose phosphate pathways in chloroplasts and the cytosol. My findings and regulatory properties of these pathways are consistent with observations of lower-than-expected increases of photosynthesis in response to increasing C_a . Reported advances in understanding leaf respiratory mechanisms may enable modelling and prediction of respiration effects (*inter alia*) on biosphere-atmosphere CO₂ exchange and plant performance under climate change.

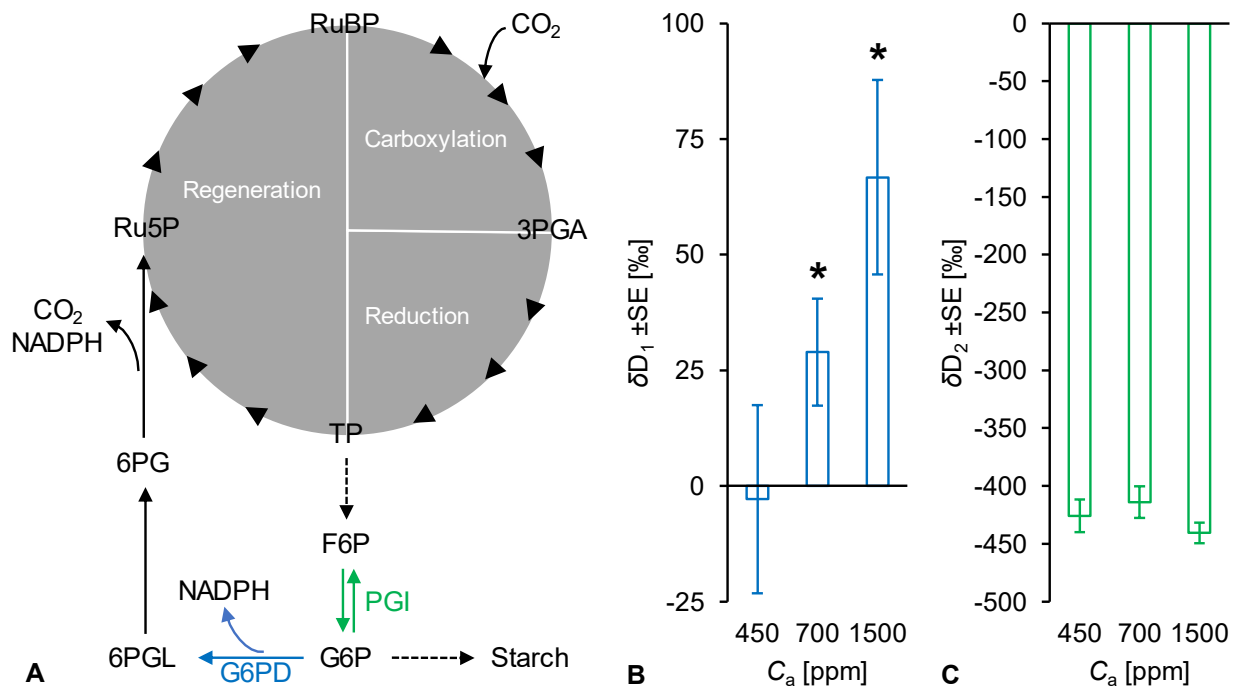


Figure 1 (A) Oxidative pentose phosphate pathway in chloroplasts carrying anaplerotic flux into the Calvin-Benson cycle (grey). Blue and green: Enzyme reactions that introduce deuterium fractionation signals at glucose H¹ and H², respectively. Dashed arrows: Intermediate reactions not shown. The cytosolic oxidative pentose phosphate pathway (not shown) starts from TP that was exported to the cytosol by the triose phosphate translocator (Fliege *et al.*, 1978). Synthesised pentose phosphate is reimported into chloroplasts by the pentose phosphate translocator (Eicks *et al.*, 2002). Enzymes: G6PD, glucose-6-phosphate dehydrogenase; PGI, phosphoglucomutase isomerase. Metabolites: 3PGA, 3-phosphoglycerate; 6PG, 6-phosphogluconate; 6PGL, 6-phosphogluconolactone; F6P, fructose 6-phosphate; G6P, glucose 6-phosphate; NADPH, nicotinamide adenine dinucleotide phosphate; Ru5P, ribulose 5-phosphate; RuBP, ribulose 1,5-bisphosphate; TP, triose phosphates (glyceraldehyde 3-phosphate, dihydroxyacetone phosphate). Modified figure from Wieloch *et al.* (2022b). **(B, C)** Deuterium abundance at glucose H¹ (blue bars), and H² (green bars) of sunflower leaf starch. Asterisks denote deuterium abundances that are significantly greater than zero (one-tailed one-sample t-test: $p < 0.05$, $n = 5$). The plants were raised in chambers over 7 to 8 weeks at $C_a = 450$ ppm. After a day in darkness to drain the starch reserves, the plants were grown for two days at different levels of C_a (450, 700, 1500 ppm) corresponding to different levels of C_i (328, 531, 1365 ppm). Data expressed as $\delta D_1 = D_1/D_{6S}-1$ and $\delta D_2 = D_2/D_{6R}-1$ where D_i denotes relative deuterium abundances at specific carbon-bound hydrogens of glucose. Deuterium abundances at glucose H^{6S} and H^{6R} are used as references because glucose H¹ and H^{6S} and H² and H^{6R} have the same precursors at the chloroplast triose-phosphate level, and H^{6S} and H^{6R} are not modified in the starch biosynthesis pathway (Wieloch *et al.*, 2022a).

Anaplerotic flux and associated respiration increase at high C_a

In contrast to $C_a = 450$ ppm, δD_1 is significantly greater than zero at $C_a = 700$ ppm (29‰) and $C_a = 1500$ ppm (67‰) (Fig. 1B; one-tailed one-sample t-test: $p < 0.05$, $n=5$). This is consistent with significant anaplerotic flux into the CBC. By contrast, δD_2 exhibits low values of around -427‰ at $C_a \geq 450$ ppm (Fig. 1C) indicating that the PGI reaction remains stably removed from equilibrium on the side of fructose 6-phosphat (F6P) (cf. Wieloch *et al.*, 2022a). The absence of a δD_2 response is remarkable because anaplerotic flux was proposed to be controlled at the level of PGI (Sharkey & Weise, 2016). Accordingly, we previously observed simultaneous shifts of δD_1 and δD_2 for C_a shifts below 450 ppm (Figure S1) (Wieloch *et al.*, 2022a). Thus, the results suggest regulatory differences of the anaplerotic pathway for low and high C_a conditions.

In the light, chloroplast G6PD is inhibited by redox regulation via thioredoxin (Née *et al.*, 2009), yet inhibition may be reversed allosterically by increasing concentrations of glucose 6-phosphate (G6P) (Cossar *et al.*, 1984; Preiser *et al.*, 2019). At medium C_a , the PGI reaction in chloroplasts is strongly removed from equilibrium on the side of F6P resulting in low [G6P]/[F6P] ratios and G6P concentrations (Dietz, 1985; Gerhardt *et al.*, 1987; Kruckeberg *et al.*, 1989; Schleucher *et al.*, 1999). Low G6P concentrations are believed to restrict the anaplerotic flux (Sharkey & Weise, 2016). Towards low C_a , G6P concentrations increase more than F6P concentrations, i.e., the PGI reaction shifts towards equilibrium (Dietz, 1985). Towards high C_a , [G6P]/[F6P] ratios remain low, yet F6P and G6P concentrations both increase along with net carbon assimilation (Dietz, 1985). Thus, towards low C_a , G6P concentrations and anaplerotic flux increase due to regulation at PGI. By contrast, increases towards high C_a are not caused by regulation at PGI but probably by increases in net carbon assimilation and concomitantly increasing G6P concentrations.

Estimation of anaplerotic flux and associated respiration at high C_a

A previously published model describing hydrogen isotope fractionation by G6PD can be used to estimate anaplerotic flux into the CBC, associated respiration, and NADPH supply (Wieloch *et al.*, 2022a). At $C_a = 700$ ppm, $\approx 4.2\%$ of the G6P entering the starch biosynthesis pathway is diverted into the anaplerotic pathway while it is $\approx 9.4\%$ at 1500 ppm. Assuming 50% of all net assimilated carbon becomes starch (Sharkey *et al.*, 1985), anaplerotic respiration proceeds at $\approx 2\%$ and $\approx 5\%$ relative to net carbon assimilation at $C_a = 700$ and 1500 ppm, respectively. These

estimates are based on δD_1 signal strengths in starch glucose. At medium to high C_a , the PGI reaction is on the side of F6P (Fig. 1C) (Dietz, 1985). To a degree, this prevents conversion of G6P (the site of signal introduction) back to F6P. F6P may leave the starch biosynthesis pathway via transketolase causing signal washout (Wieloch *et al.*, 2022a). At low C_a , the PGI reaction is closer to or at equilibrium and signal washout can be expected to be significant (Notes S1) (Wieloch *et al.*, 2022a). Thus, the G6PD fractionation model may significantly underestimate anaplerotic flux at low C_a , while high- C_a estimates can be expected to be closer to actual values.

Potential causes of lower-than-expected increases of photosynthesis in response to increasing C_a

In C_3 plants, net carbon assimilation increases with increasing C_a (Drake *et al.*, 1997; Ainsworth & Long, 2005). However, responses seen in FACE experiments differ significantly among plant functional groups with trees showing the strongest increase (Nowak *et al.*, 2004; Ainsworth & Long, 2005). Hence, some plant functional groups apparently come closer to theoretically possible increases calculated from rubisco kinetics than others (Long, 1991). As shown above, anaplerotic flux increases with increasing C_a . Thus, respiration by the anaplerotic pathway can explain part of the lower-than-expected increase of net carbon assimilation by C_a .

Another part may be explained by respiration by the cytosolic OPPP. Primary control of flux through this pathway is exerted at the level of its first enzyme, G6PD. In the light, cytosolic G6PD activity in potato leaf discs was shown to increase with increasing glucose concentration through *de novo* enzyme synthesis (Hauschild & von Schaewen, 2003). In arabidopsis rosettes, 88% of the glucose was shown to be in the vacuole and cytosol (Szecowka *et al.*, 2013). As part of sucrose cycling, cytosolic hexokinase converts this glucose into G6P (Dancer *et al.*, 1990; Xu *et al.*, 2022). G6P-derived carbon can re-enter the CBC via the cytosolic OPPP (Eicks *et al.*, 2002; Xu *et al.*, 2022). Combinedly, sucrose cycling and flux through the cytosolic OPPP can explain ^{13}C labelling lags of CBC metabolites (Sharkey *et al.*, 2020; Xu *et al.*, 2022). These authors estimate that respiration by the cytosolic OPPP proceeds at $\approx 5\%$ relative to the rate of net carbon assimilation in poplar at 30 °C and in camelina at 22 °C. Since ^{13}C labelling lags of CBC metabolites appear to occur generally (Mahon *et al.*, 1974; Canvin, 1979; Hasunuma *et al.*, 2010; Szecowka *et al.*, 2013; Ma *et al.*, 2014; Sharkey *et al.*, 2020; Xu *et al.*, 2022) and since, by supplying cytosolic NADPH,

the OPPP fulfils an important physiological function (Wieloch & Sharkey, 2022), substantial OPPP respiration is likely a general feature of C₃ plants. Previously, Tjoelker *et al.* (2009) reported a positive linear relationship between respiration at 5 °C and leaf soluble sugar concentration in illuminated pine needles ($R^2 = 0.49$, $p < 10^{-4}$, $n = 40$). In their study, soluble sugar concentration denotes the average concentration of raffinose, sucrose, glucose, and fructose. Reanalysing the data of Tjoelker *et al.* (2009), I find a positive linear relationship between respiration at 5 °C and glucose concentration (Fig. 2, $R^2 = 0.88$, $p < 10^{-6}$, $n = 15$, red cross: outlier removed prior to analysis; see Fig. 2 caption for information on materials and methods). Leaf soluble sugar concentration generally increases with increasing C_a (Ainsworth & Long, 2005). Taken together, these data may suggest that, as C_a increases, leaf glucose concentration increases causing increased expression of cytosolic G6PD, and flux through the cytosolic OPPP. Associated respiration may explain part of the lower-than-expected increase of net carbon assimilation by C_a .

Compared to other plant functional groups, trees exhibit stronger increases in net carbon assimilation in response to increasing C_a (Ainsworth & Long, 2005) and are thus getting closest to theoretically possible increases (Long, 1991). However, the additional carbon does not result in stronger increases in leaf soluble sugar concentration. On the contrary, trees exhibit lower increases in leaf soluble sugar concentration than other plant functional groups (Ainsworth & Long, 2005). By contrast, trees exhibit the highest increase in dry matter accumulation (Ainsworth & Long, 2005). Thus, low increases in leaf soluble sugar concentration are probably explained by high sink strengths of the relatively young and fast-growing trees studied in FACE experiments. In turn, low increases in leaf soluble sugar concentration may cause low increases in respiration by both the plastidial and cytosolic OPPP (see above). This may explain why trees come closer to theoretically possible increases in net carbon assimilation in response to C_a than other plant functional groups. Overall, based on analyses and argumentation presented here, increases of net carbon assimilation by increasing C_a (including acclimation effects) may depend on plant sink strength and associated OPPP respiration.

OPPP flux in chloroplasts introduces a δD_1 signal in starch (see above). Similarly, OPPP flux in the cytosol of leaves can be expected to introduce a δD_1 signal in the glucosyl and fructosyl moieties of sucrose. These signals will be recorded in tree-ring glucose because it is synthesised

from starch and sucrose. However, signal interpretation will be complicated by several processes including signal washout in chloroplasts (see above) and OPPP flux and triose phosphate cycling in the cytosol of tree-ring cells. Nevertheless, I believe these complications can be addressed and encourage the development of δD_1 signal analysis to retrieve information about leaf respiration and respiratory acclimation to increasing C_a from leaf, phloem, and tree-ring metabolites.

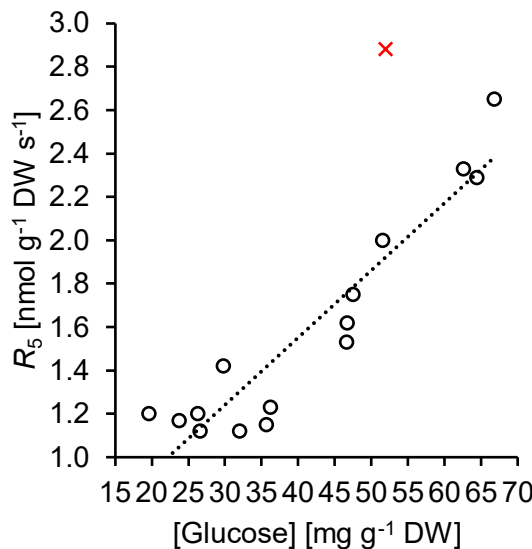


Figure 2 Respiration at 5 °C (R_5) as function of glucose concentration in illuminated needles of 33-yr-old *Pinus banksiana*. Dotted line: positive linear relationship between both variables ($R^2 = 0.88$, $p < 10^{-6}$, $n = 15$). Red cross: outlier removed prior to regression analysis. Data collected from eight provenances (boreal to temperate origin, 44 to 55 °N) grown in a common garden in Cloquet, MN, USA. Sun-exposed canopy branch sampled from four randomly selected trees per provenance at two dates, one in mid-November 1997 and one in mid-May 1998. R_5 measured in a laboratory at $C_a \approx 380$ ppm within 6 h after sampling by infrared gas analysers and cuvettes (LCA-3 and PLC-C, Analytical Development Co. Ltd, Hoddesdon, UK). Note, respiration was shown to remain stable over several hours after sampling (Mitchell *et al.*, 1999; Ow *et al.*, 2008; Tjoelker *et al.*, 2009). Glucose concentration measured by HPLC (Waters Associates, Milford, MA, USA) equipped with a Sugar Pack I column and a refractive index detector (Waters 410) following published procedures (Pukacka & Pukacki, 1997). Soluble sugar extracted from dried needles used as starting material. Figure shows data published by Tjoelker *et al.* (2009). For further information on material and methods, see Tjoelker *et al.* (2009).

A paradigm shift in the field of leaf day respiration?

In the past, research of leaf day respiration had a strong focus on mitochondrial processes. However, according to recent analyses of metabolic fluxes in leaves of *Arabidopsis thaliana* and *Camelina sativa*, mitochondrial respiration is relatively low (1 to 1.6% relative to the rate of net carbon assimilation) (Ma *et al.*, 2014; Xu *et al.*, 2022). By contrast, respiration by the cytosolic OPPP is \approx 5% relative to the rate of net carbon assimilation in *Camelina sativa* leaves (Xu *et al.*, 2022). Similarly, in sunflower leaves, respiration by the OPPP in chloroplasts is relatively high under both high (see above) and low C_a (Notes S1) (Wieloch *et al.*, 2021a, 2022a). These findings indicate that the OPPP may be more important for overall leaf day respiration than mitochondrial processes.

Data availability

The data supporting the findings of this study have been published previously (Tjoelker *et al.*, 2009; Wieloch *et al.*, 2022a).

Competing interest statement: The author declares no competing interests.

References

Ainsworth EA, Long SP. 2005. What have we learned from 15 years of free-air CO₂ enrichment (FACE)? A meta-analytic review of the responses of photosynthesis, canopy properties and plant production to rising CO₂. *New Phytologist* **165**: 351–372.

Canvin DT. 1979. Photorespiration: Comparison between C₃ and C₄ plants. In: Gibbs M, Latzko E, eds. *Photosynthesis II: Photosynthetic Carbon Metabolism and Related Processes*. Berlin, Heidelberg: Springer Berlin Heidelberg, 368–396.

Cossar JD, Rowell P, Stewart WDP. 1984. Thioredoxin as a modulator of glucose-6-phosphate dehydrogenase in a N₂-fixing cyanobacterium. *Microbiology* **130**: 991–998.

Dancer J, Hatzfeld W-D, Stitt M. 1990. Cytosolic cycles regulate the turnover of sucrose in heterotrophic cell-suspension cultures of *Chenopodium rubrum* L. *Planta* **182**: 223–231.

Dietz K-J. 1985. A possible rate-limiting function of chloroplast hexosemonophosphate isomerase in starch synthesis of leaves. *Biochimica et Biophysica Acta* **839**: 240–248.

Drake BG, González-Meler MA, Long SP. 1997. More efficient plants: A consequence of rising atmospheric CO₂? *Annual Review of Plant Physiology and Plant Molecular Biology* **48**: 609–639.

Dusenge ME, Duarte AG, Way DA. 2019. Plant carbon metabolism and climate change: elevated CO₂ and temperature impacts on photosynthesis, photorespiration and respiration. *New Phytologist* **221**: 32–49.

Ehlers I, Augusti A, Betson TR, Nilsson MB, Marshall JD, Schleucher J. 2015. Detecting long-term metabolic shifts using isotopomers: CO₂-driven suppression of photorespiration in C₃ plants over the 20th century. *Proceedings of the National Academy of Sciences of the United States of America* **112**: 15585–15590.

Eicks M, Maurino V, Knappe S, Flügge U-I, Fischer K. 2002. The plastidic pentose phosphate translocator represents a link between the cytosolic and the plastidic pentose phosphate pathways in plants. *Plant Physiology* **128**: 512–522.

Fliege R, Flügge UI, Werdan K, Heldt HW. 1978. Specific transport of inorganic phosphate, 3-phosphoglycerate and triosephosphates across the inner membrane of the envelope in spinach chloroplasts. *Biochimica et Biophysica Acta* **502**: 232–247.

Gerhardt R, Stitt M, Heldt HW. 1987. Subcellular metabolite levels in spinach leaves: Regulation of sucrose synthesis during diurnal alterations in photosynthetic partitioning. *Plant Physiology* **83**: 399–407.

González-Meler MA, Taneva L, Trueman RJ. 2004. Plant respiration and elevated atmospheric CO₂ concentration: Cellular responses and global significance. *Annals of Botany* **94**: 647–656.

Hasunuma T, Harada K, Miyazawa S-I, Kondo A, Fukusaki E, Miyake C. 2010. Metabolic turnover analysis by a combination of *in vivo* ¹³C-labelling from ¹³CO₂ and metabolic profiling with CE-MS/MS reveals rate-limiting steps of the C₃ photosynthetic pathway in *Nicotiana tabacum* leaves. *Journal of Experimental Botany* **61**: 1041–1051.

Hauschild R, von Schaewen A. 2003. Differential regulation of glucose-6-phosphate dehydrogenase isoenzyme activities in potato. *Plant Physiology* **133**: 47–62.

Kruckeberg AL, Neuhaus HE, Feil R, Gottlieb LD, Stitt M. 1989. Decreased-activity mutants of phosphoglucose isomerase in the cytosol and chloroplast of *Clarkia xantiana*. *The Biochemical Journal* **261**: 457–467.

Long SP. 1991. Modification of the response of photosynthetic productivity to rising temperature by atmospheric CO₂ concentrations: Has its importance been underestimated? *Plant, Cell & Environment* **14**: 729–739.

Ma F, Jazmin LJ, Young JD, Allen DK. 2014. Isotopically nonstationary ¹³C flux analysis of changes in *Arabidopsis thaliana* leaf metabolism due to high light acclimation. *Proceedings of the National Academy of Sciences of the United States of America* **111**: 16967–16972.

Mahon JD, Fock H, Canvin DT. 1974. Changes in specific radioactivity of sunflower leaf metabolites during photosynthesis in ¹⁴CO₂ and ¹²CO₂ at three concentrations of CO₂. *Planta* **120**: 245–254.

Mitchell KA, Bolstad PV, Vose JM. 1999. Interspecific and environmentally induced variation in foliar dark respiration among eighteen southeastern deciduous tree species. *Tree Physiology* **19**: 861–870.

Née G, Zaffagnini M, Trost P, Issakidis-Bourguet E. 2009. Redox regulation of chloroplastic glucose-6-phosphate dehydrogenase: A new role for f-type thioredoxin. *FEBS Letters* **583**: 2827–2832.

Nowak RS, Ellsworth DS, Smith SD. 2004. Functional responses of plants to elevated atmospheric CO₂ – do photosynthetic and productivity data from FACE experiments support early predictions? *New Phytologist* **162**: 253–280.

Ow LF, Griffin KL, Whitehead D, Walcroft AS, Turnbull MH. 2008. Thermal acclimation of leaf respiration but not photosynthesis in *Populus deltoides* × *nigra*. *New Phytologist* **178**: 123–134.

Preiser AL, Fisher N, Banerjee A, Sharkey TD. 2019. Plastidic glucose-6-phosphate dehydrogenases are regulated to maintain activity in the light. *Biochemical Journal* **476**: 1539–1551.

Pukacka S, Pukacki PM. 1997. Changes in soluble sugars in relation to desiccation tolerance and effects of dehydration on freezing characteristics of *Acer platanoides* and *Acer pseudoplatanus* seeds. *Acta Physiologiae Plantarum* **19**: 147–154.

Schleucher J, Vanderveer P, Markley JL, Sharkey TD. 1999. Intramolecular deuterium distributions reveal disequilibrium of chloroplast phosphoglucose isomerase. *Plant, Cell and Environment* **22**: 525–533.

Sharkey TD, Berry JA, Raschke K. 1985. Starch and sucrose synthesis in *Phaseolus vulgaris* as affected by light, CO₂, and abscisic acid. *Plant Physiology* **77**: 617–620.

Sharkey TD, Preiser AL, Weraduwage SM, Gog L. 2020. Source of ¹²C in Calvin-Benson cycle intermediates and isoprene emitted from plant leaves fed with ¹³CO₂. *The Biochemical Journal* **477**: 3237–3252.

Sharkey TD, Weise SE. 2016. The glucose 6-phosphate shunt around the Calvin–Benson cycle. *Journal of Experimental Botany* **67**: 4067–4077.

Szecowka M, Heise R, Tohge T, Nunes-Nesi A, Vosloh D, Huege J, Feil R, Lunn J, Nikoloski Z, Stitt M, et al. 2013. Metabolic fluxes in an illuminated *Arabidopsis* rosette. *The Plant Cell* **25**: 694–714.

Tjoelker MG, Oleksyn J, Lorenc-Plucinska G, Reich PB. 2009. Acclimation of respiratory temperature responses in northern and southern populations of *Pinus banksiana*. *New Phytologist* **181**: 218–229.

Way DA, Oren R, Kroner Y. 2015. The space-time continuum: the effects of elevated CO₂ and temperature on trees and the importance of scaling. *Plant, Cell & Environment* **38**: 991–1007.

Wieloch T, Augusti A, Schleucher J. 2021a. Anaplerotic flux into the Calvin-Benson cycle. Integration in carbon and energy metabolism of *Helianthus annuus*. *bioRxiv*: 2021.07.30.454461.

Wieloch T, Augusti A, Schleucher J. 2022a. Anaplerotic flux into the Calvin-Benson cycle. Hydrogen isotope evidence for *in vivo* occurrence in C₃ metabolism. *New Phytologist* **234**: 405–411.

Wieloch T, Ehlers I, Yu J, Frank D, Grabner M, Gessler A, Schleucher J. 2018. Intramolecular ¹³C analysis of tree rings provides multiple plant ecophysiology signals covering decades. *Scientific Reports* **8**: 5048.

Wieloch T, Grabner M, Augusti A, Serk H, Ehlers I, Yu J, Schleucher J. 2022b. Metabolism is a major driver of hydrogen isotope fractionation recorded in tree-ring glucose of *Pinus nigra*. *New Phytologist* **234**: 449–461.

Wieloch T, Sharkey TD. 2022. Compartment-specific energy requirements of photosynthetic carbon metabolism in *Camelina sativa* leaves. *Planta* **255**: 103.

Wieloch T, Sharkey TD, Werner RA, Schleucher J. 2022c. Intramolecular carbon isotope signals reflect metabolite allocation in plants. *Journal of Experimental Botany* **73**: 2558–2575.

Wieloch T, Werner RA, Schleucher J. 2021b. Carbon flux around leaf-cytosolic glyceraldehyde-3-phosphate dehydrogenase introduces a ¹³C signal in plant glucose. *Journal of Experimental Botany* **72**: 7136–7144.

Xu Y, Wieloch T, Kaste Joshua AM, Shachar-Hill Y, Sharkey TD. 2022. Reimport of carbon from cytosolic and vacuolar sugar pools into the Calvin-Benson cycle explains photosynthesis labeling anomalies. *Proceedings of the National Academy of Sciences of the United States of America* **119**: e2121531119.